Further Radiochemical Studies of the High-Energy Fission Products*

P. C. Stevenson, H. G. Hicks, W. E. Nervik, and D. R. Nethaway
University of California Radiation Laboratory, Livermore, California
(Received April 11, 1958)

Formation cross sections of various U^{238} fission products have been measured as a function of bombarding-particle energy, using protons (10–340 Mev) and deuterons (20–190 Mev). The reactions $Al^{27}(p,3pn)Na^{24}$ and $Al^{27}(d,\alpha p)Na^{24}$ were used as monitoring reactions to measure effective cyclotron beam intensity. Fission-product distribution curves and total fission cross sections have been measured. Above 50-Mev bombarding energy, the fission-product distribution is not symmetrical about a given mass number at a given bombardment energy.

I. INTRODUCTION

PREVIOUS studies[1,2] of the high-energy charged-particle fission of U^{238} did not include examination of the yields of masses greater than 140. Formation cross sections of several rare-earth nuclides ($A = 140$ to 157), Y^{90}, Y^{91}, Y^{93}, Mo^{99}, and Ba^{140} have been measured in the present work. Proton energies range from 10 to 340 Mev; deuteron energies, from 20 to 190 Mev.

II. EXPERIMENTAL TECHNIQUES

Preparation of targets[3] and bombardment techniques[1] have been described previously by some of the authors. The cyclotron beam intensity was monitored using the reactions $Al^{27}(p,3pn)Na^{24}$ (70 to 340 Mev) or Al^{27}-$(d,\alpha p)Na^{24}$ (28 to 190 Mev) in aluminum foils surrounding the targets, as described previously[1-3]; the published cross sections of Hicks, Stevenson, and Nervik[3] and of Batzel, Crane, and O'Kelly[4] were used. Beam intensities were measured by means of a Faraday cup when bombardments were made using 10- and 32-Mev protons and 20-Mev deuterons.

Radiochemical determination of Mo^{99} was performed in the manner described by Gunn et al.,[5] and the method of isolation and separation of rare earths and yttrium was performed in the manner described by Nervik.[6] The Ba^{140} was purified by repeated precipitation of the chloride from diethyl ether-hydrochloric acid mixtures and by scavenging with ferric and lanthanum hydroxides.

Gamma and bremsstrahlung radiations from all nuclides measured, except Mo^{99}, were counted by means of a NaI(Tl) scintillation crystal, with the lower discriminator set at 20 kev and the upper discriminator set at 3 Mev. Sufficient beryllium (2 g/cm²) to stop all beta particles was interposed between the counting sample and crystal. The counting of the gamma and bremsstrahlung radiations by-passed the problem of

beta scattering, for experiments have shown that under these conditions there is no significant variation of observed specific activity with mass thickness of sample. The counting efficiency of each nuclide was determined by relating the observed counting rate of a carrier-free sample in the scintillation crystal counters to that in a 4π-geometry beta counter. Several determinations were made for each species and the agreement between duplicate determinations was excellent.

The nuclide Mo^{99} was counted with an end-window, continuous-flow methane proportional counter. The counting efficiency was determined indirectly by means of fission counting (described in reference 5) and the accepted thermal-neutron fission yield of Mo^{99}, 6.10%.[7] The formation cross sections are summarized in Figs. 1 and 2 and Tables I and II. The agreement with previous data[1,2,8] is good.

III. DISCUSSION OF RESULTS

The data (Figs. 1 and 2 and Tables I and II) show features reported by previous authors.[1,2,8-13] As the bombarding energy increases, modes of fission that are extremely improbable in low-energy-induced fission become increasingly important. This results in an increase of fission yield for species formed by symmetric fission and for extremely asymmetric fission, as well as increased direct formation of species near or even on the light-mass side of the beta-stability region.

In drawing smooth curves through the observed fission yield values, an interesting phenomenon was observed. Below 50-Mev proton or deuteron energy the curves are symmetrical in all respects. Above 50 Mev, however, they are very definitely not symmetrical. Reflection of the heavy rare-earth cross sections through the "apparent center of the fission yield curve" as estimated from higher-yield products gives points that

* This work was performed under the auspices of the U. S. Atomic Energy Commission.
[1] Hicks, Stevenson, Gilbert, and Hutchin, Phys. Rev. **100**, 1284 (1955).
[2] H. G. Hicks and R. S. Gilbert, Phys. Rev. **100**, 1286 (1955).
[3] Hicks, Stevenson, and Nervik, Phys. Rev. **102**, 1390 (1956).
[4] Batzel, Crane, and O'Kelly, Phys. Rev. **91**, 939 (1953).
[5] Gunn, Hicks, Stevenson, and Levy, Phys. Rev. **107**, 1642 (1957).
[6] W. E. Nervik, J. Phys. Chem. **59**, 690 (1955).

[7] J. O. Blomeke, Oak Ridge National Laboratory Report ORNL-1783, November 2, 1955 (unpublished).
[8] M. Lindner and R. N. Osborne, Phys. Rev. **94**, 1323 (1954).
[9] R. W. Spence and G. P. Ford, *Annual Review of Nuclear Science* (Annual Reviews, Inc., Stanford, 1953), Vol. 2, p. 399.
[10] R. H. Goeckermann and I. Perlman, Phys. Rev. **76**, 628 (1949).
[11] P. R. O'Connor and G. T. Seaborg, Phys. Rev. **74**, 1189 (1948).
[12] Folger, Stevenson, and Seaborg, Phys. Rev. **98**, 107 (1955).
[13] E. M. Douthett and D. H. Templeton, Phys. Rev. **94**, 128 (1954).

TABLE I. Formation cross sections in millibarns for products of U^{238} fission with protons.

Nuclide \ Energy (Mev)	10	32	70	100	150	200	250	300	340
Y^{90} [a]	...	0	0.02	0.11	0.15	3.7	3.8	3.9	7.2
Y^{91}	0.34	27	27	30	27	26	37	37	32
Y^{93}	0.80	43	...	49	39	38	38	38	38
Mo^{99}	1.9	62	71	69	55	53	58	62	59
La^{140} [a]	...	2.8	8.6	8.6	7.9	6.2	7.3	7.0	5.5
Ce^{141}	1.7	48	49	51	36	36	...	...	31
Ce^{143}	1.2	45	36	31	22	21	21	23	20
Pr^{143} [a]	0	0	0.36	2.1	2.0	1.9	2.2	2.3	1.9
Ce^{144}	1.1	35	30	28	18	17	...	...	14
Nd^{140} [b]	...	...	0	0	0.7	3.4	7.1	13	17
Nd^{147}	0.60	17	17	18	12	11.3	11.4	10.8	9.7
Sm^{153}	0.12	4.2	4.6	4.4	3.1	2.6	2.6	2.4	2.0
Eu^{156}	0.02	1.12	1.22	1.31	0.93	0.86	0.92	1.12	1.22
Eu^{157}	0.02	0.69	0.90	0.89	0.54	0.46	0.47	0.42	0.40

[a] Independent formation cross section.
[b] Relative values, i.e., the counting efficiency is unknown.

fall well below the observed values of the low-mass-number wing of the curve. On the other hand, reflection of the low-mass-number cross sections through the same "apparent center" mass A gives points that fall above the observed rare-earth values. The higher the energy of the bombarding particle, the more pronounced the effect. The cross sections of Cu^{67} and Ni^{66} with 340-Mev protons, for example, must be adjusted downward by at least an order of magnitude, or those of Eu^{156} and Eu^{157} adjusted upward by factors of from three to seven, in order to fall on a curve symmetric about a single A. Duplicate runs of Eu^{156} and Eu^{157} cross sections showed agreement within five percent, while the cross sections of Cu^{67} and Ni^{66} were from independent investigations.[8] The effect is certainly outside of experimental error.

The phenomenon described above might conceivably come about if a major portion of the independent yields of the rare-earth nuclides arose from direct formation either as stable isotopes or on the neutron-deficient side of stability. If the primary fission products of mass 156, for instance, were distributed so that 75–80% of the mass yield lay in the region where $Z \geq 64$ (Gd or higher), then the fission yield curves could be considered to be symmetric. This situation appeared unlikely, for only one neutron-deficient species (Nd^{140}) was detected in the entire rare-earth region. More conclusively, if the major portion of the yield of mass 156 lay in the region $Z \geq 64$, then the direct-formation cross section of Eu^{156} should have been of magnitude comparable to or larger than that of Sm^{156}. Measurement of the direct-formation cross section of Eu^{156} showed that over 90% of the Eu^{156} was formed from its Sm^{156} parent by beta decay. Thus, the fission yield distribution above 50 Mev is not symmetrical.

The fission cross sections shown in Figs. 3 and 4 and Table III were obtained by integration under the fission-yield curves. Also shown are the data of previous

TABLE II. Formation cross sections in millibarns for products of U^{238} fission with deuterons.

Nuclide \ Energy (Mev)	20	28	50	75	100	125	150	170	190
Y^{90} [a]	...	0	<0.01	0.083	0.55	1.4	2.1	2.8	3.4
Y^{91} [a]	...	20	4.7	9.5	10	11	12	12	12
Y^{91}	19	20	22	38	42	45	48	50	51
Y^{93}	24	25	46	65	71	65	62	65	68
Mo^{99}	55	60	68	92	101	97	92	92	92
La^{140} [a]	...	0.44	4.0	10	12	12	10	11	11
La^{141}	28	30	54	71	67	59	50	53	53
Ce^{141} [a]	...	0	0	0	4.5	8.0	8.5	7.0	6.5
Ce^{143}	22	28	37	49	46	40	36	35	35
Pr^{143} [a]	...	0	0	0.52	1.5	2.7	2.9	3.2	3.1
Ce^{144}	20	25	33	43	39	32	28	29	28
Nd^{140} [b]	...	<0.2	<0.2	<0.2	<0.2	<0.2	0.5	1	3
Nd^{147}	11	12	22	29	27	24	21	20	20
Sm^{153}	2.5	2.7	5.7	7.2	7.0	6.0	5.0	4.8	4.7
Eu^{156}	0.60	0.67	1.5	2.0	2.1	1.9	1.6	1.6	1.6
Eu^{157}	0.50	0.61	1.0	1.5	1.4	1.1	1.0	1.0	0.87

[a] Independent formation cross section.
[b] Relative values, i.e., the counting efficiency is unknown.
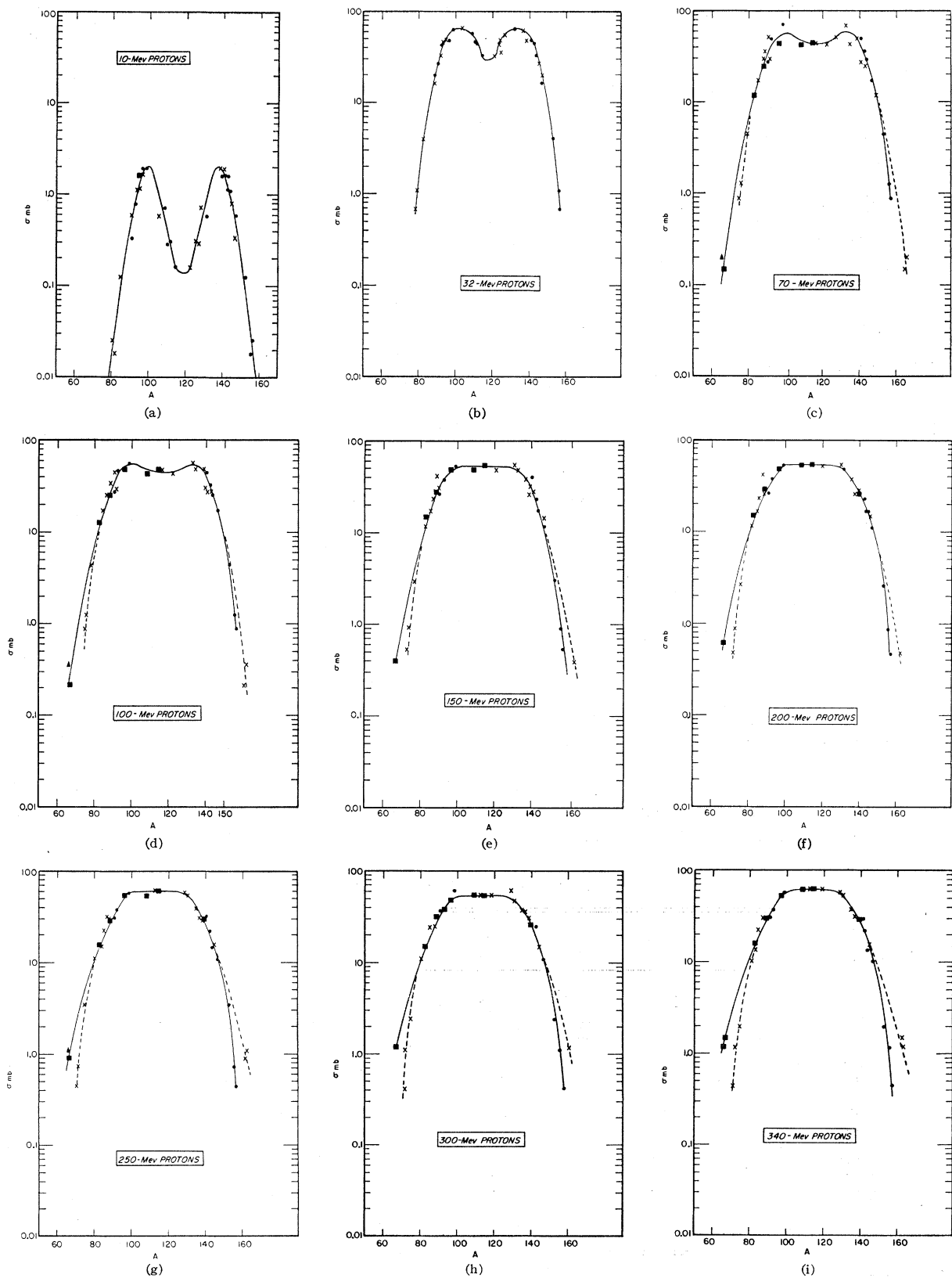
FIG. 1. Fission-product distributions of U^{238} bombarded with protons of various energies. The symbol ● denotes present work; ■ denotes previous work by Hicks, Stevenson, Gilbert and Hutchin[1,2]; ▲ denotes work by Lindner and Osborne[3]; and ✗ denotes reflection points.
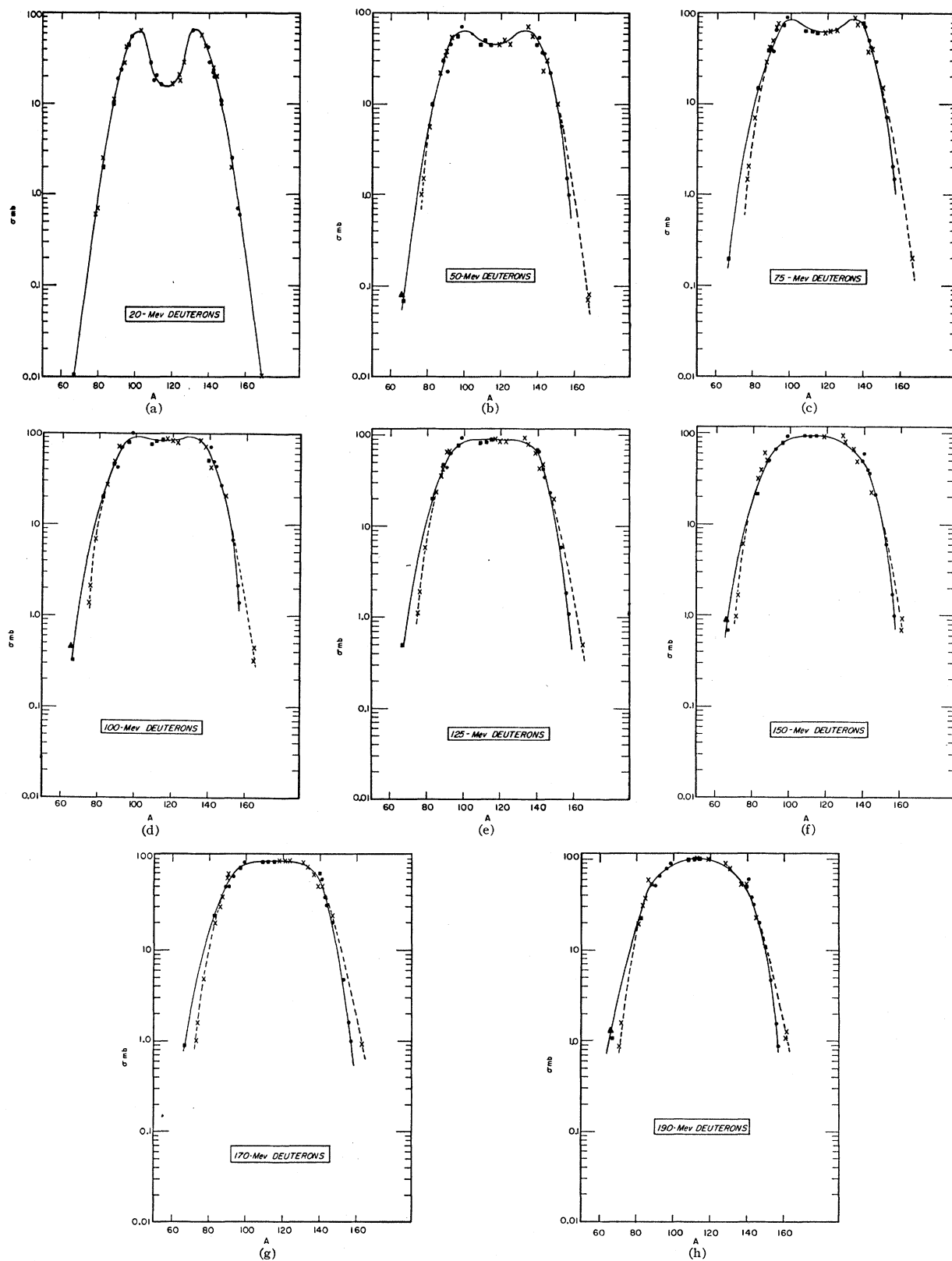
FIG. 2. Fission-product distributions of U^{238} bombarded with deuterons of various energies. The symbol ● denotes present work; ■ denotes previous work by Hicks, Stevenson, Gilbert, and Hutchin[1,2]; ▲ denotes work by Lindner and Osborne[3]; and ✕ denotes reflection points.
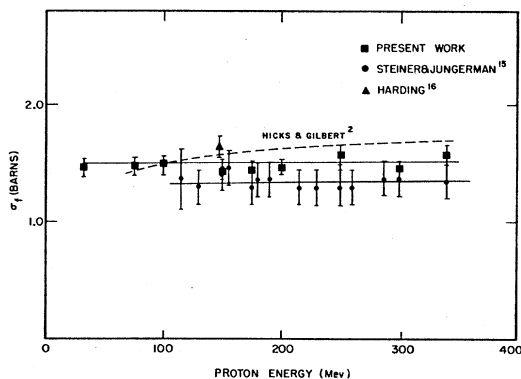
FIG. 3. Fission cross section of U^{238} bombarded with protons of various energies.

workers.[14-16] The differences between the present work and that of reference 2 reflects the error of the assumption that the fission-product distribution is symmetrical.

As the energy of the bombarding particles is increased above 30–40 Mev, the mean free path of the projectile in nuclear matter becomes comparable to the diameter of the target nucleus, rendering the nucleus partially transparent to high-energy nucleons.[17] The picture of, "compound nucleus" formation must be abandoned and collisions of the projectile with individual nucleons in the target nucleus must be considered. In each of the collisions, the energy transfer to the nucleus is a fraction of the projectile energy. The total energy transferred to the nucleus then depends on the number of collisions the projectile makes within the nucleus and may vary from the full energy of the projectile to a small fraction thereof.
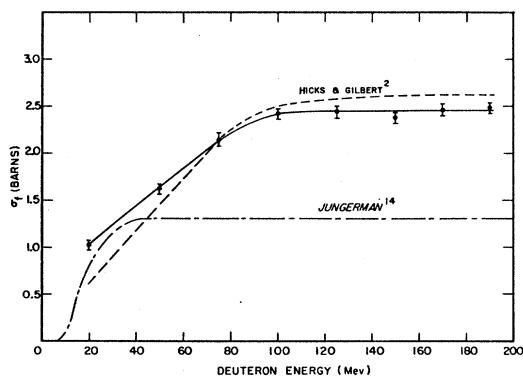
FIG. 4. Fission cross section of U^{238} bombarded with deuterons of various energies.

[14] J. A. Jungerman, Phys. Rev. 79, 632 (1950).
[15] H. M. Steiner and J. A. Jungerman, Phys. Rev. 101, 807 (1956).
[16] G. N. Harding, Atomic Energy Research Establishment Report AERE/NR-1438, Harwell, Berkshire, England, June, 1954 (unpublished).
[17] R. Serber, Phys. Rev. 72, 1114 (1947).

Monte Carlo calculations by Turkevich on the deposition of energy in the Bi^{209} nucleus by protons appear in an article by Porile and Sugarman.[18] The results show that the majority of the interactions deposit less than half the projectile energy at 286 and 458 Mev.

When the transfer of energy to the nucleus is small, comparatively few nucleons are evaporated either before or after fission and the sum of the complementary-fragment mass numbers is close to 238. Similarly, when the energy transfer is large, the system evaporates many nucleons, predominately neutrons, and the sum of the complementary-fission-fragment mass numbers is much less than 238. The lower-energy fission events are characterized by a saddle in the central region $(A \sim 118)$ of the distribution curve symmetric about a given A, and by very steep sides in the low- and high-A regions. As the bombarding energy increases, the valley disappears and the low-A wing has a lower slope than the high-A wing. From the character of the fission yield distribution at higher

TABLE III. U^{238} fission cross sections, in barns.

Protons		Deuterons	
Energy (Mev)		Energy (Mev)	
10	0.029	20	1.03
32	1.47	50	1.61
70	1.47	75	2.13
100	1.49	100	2.42
150	1.44	125	2.45
200	1.47	150	2.39
250	1.58	170	2.48
300	1.46	190	2.49
340	1.59		

energies, one may infer that for "mono-energetic" high-energy fission the valley has all but disappeared and the axis of symmetry of the distribution has shifted toward lower A. The measured distribution is, of course, a mixture of both high- and low-energy events. The fission-yield distributions in Figs. 1 and 2 display apparent symmetry about a central mass number A in the region of $A \pm 20$ at all energies. These products are major yields of both high- and low-energy fission. Thus, almost any combination of fission-yield distributions would tend to produce a slowly varying curve in this region. The products in apparent complementary positions with respect to the observed distribution are not necessarily complementary fragments of every individual fission process. The observed yields of these products are nearly the same; therefore, any discrepancies are small and tend to be averaged out.

Those nuclides on the light-mass wing of the distribution $(A \leq 75)$ are seen in appreciable yield only in high-energy-induced fission, in particular, Cu^{67} and Ni^{66}, which are not seen in thermal-neutron or low-

[18] N. T. Porile and N. Sugarman, Phys. Rev. 107, 1422 (1957).

energy charged-particle induced fission. At 340-Mev protons, the cross sections of masses 66 and 155 are equal. Therefore, the fissioning nucleus giving rise to $A=66$ must have had enough excitation energy to lose many nucleons either before or after scission. The sum of the fission-fragment masses must be not greater than 221, and probably at least two mass units less.

On the other hand, those nuclides on the heavy-mass wing are seen in low-energy fission. The fission yield of Eu^{156} varies but slightly (from 0.06 to 0.09%) over the entire energy range of charged particles used. The slopes of all fission-product distributions in the region $A \geq 150$ (Figs. 1 and 2) are very nearly identical at all charged-particle energies used in this work.

IV. ACKNOWLEDGMENTS

Scattering of Protons in a Spin-Orbit Potential*

G. W. ERICKSON AND W. B. CHESTON
School of Physics, University of Minnesota, Minneapolis, Minnesota
(Received March 31, 1958)

An approximation method is described for treating spin-orbit potentials in the optical model. The method is essentially a perturbation expansion using exact scattering amplitudes for a central optical potential as the unperturbed scattering amplitudes. The method is compared to an exact calculation and its usefulness in the medium-energy region demonstrated. The effects of a spin-orbit term on the differential cross section and the spin polarization distribution are investigated as a function of the parameters involved in the medium-energy region. The polarization is shown to be approximately independent of the shape of the form factor of the spin-orbit term in this energy region. The reaction cross section is insensitive to the inclusion of a spin-orbit term of reasonable depth.

INTRODUCTION

EXTENSIVE analysis has been carried out in the last few years on the scattering of 10–95 Mev protons, using a central optical model potential.[1] This analysis has been moderately successful in that it has been possible to obtain angular distributions of elastically scattered protons in reasonable agreement with the experimental data although variance of the predicted angular distributions with the data at large angles and for light target nuclei is a persistent feature of the analysis. The central optical model has also been successful in understanding the total reaction cross section for medium-energy protons although the experimental data are quite meager.[2] Neither for the elastic scattering cross sections nor for the reaction cross sections is it possible to obtain a unique set of optical model parameters (i.e., depths of the real and imaginary

parts of the potential well, V and W; the falloff parameter, a; the "radius" parameter, R) which fit the experimental data. It has been conjectured by many authors that the disagreements with experiment and the ambiguity of the results of the optical model analysis using a central potential would be removed by the inclusion of spin-orbit terms in the potential. The inclusion of spin-orbit terms for bound states of protons in the nuclear shell model has, for the heavy elements, yielded real well depths in approximate agreement with those obtained by optical model analysis of scattered protons, but the falloff or surface thickness parameters so obtained are not in good agreement.[3] The analysis of scattering of 300-Mev protons using a spin-orbit potential has been recently reported.[4] Although the experimental data relevant to the properties of a proton-nucleus spin-orbit potential for intermediate-energy protons are meager except for angular distributions of elastically scattered protons, it was decided to undertake an exploration of the effects produced by a spin-orbit potential.

This study was intended to serve a variety of purposes. The examination of the effect of the spin-orbit potential on the features of the angular distribution of elastically scattered protons was undertaken

---

[1] Glassgold, Cheston, Stein, Schuldt, and Erickson, Phys. Rev. 106, 1207 (1957); Melkanoff, Moszkowski, Nodvik, and Saxon, Phys. Rev. 101, 507 (1957); A. E. Glassgold and P. J. Kellogg, Phys. Rev. 107, 1372 (1957); see also other references included in the above papers.
[2] J. T. Gooding, Bull. Am. Phys. Soc. Ser. II, 2, 350 (1957).
[3] Ross, Mark, and Lawson, Phys. Rev. 102, 1613 (1956).
[4] Bjorklund, Blandford, and Fernbach, Phys. Rev. 108, 795 (1957).